

Journal Pre-proof

A Novel General-purpose Three-dimensional Continuously Scanning Laser Doppler Vibrometer System for Full-field Vibration Measurement of a Structure with a Curved Surface

K. Yuan , W.D. Zhu

PII: S0022-460X(22)00457-6
DOI: <https://doi.org/10.1016/j.jsv.2022.117274>
Reference: YJSVI 117274



To appear in: *Journal of Sound and Vibration*

Received date: 16 May 2022
Revised date: 16 August 2022
Accepted date: 28 August 2022

Please cite this article as: K. Yuan , W.D. Zhu , A Novel General-purpose Three-dimensional Continuously Scanning Laser Doppler Vibrometer System for Full-field Vibration Measurement of a Structure with a Curved Surface, *Journal of Sound and Vibration* (2022), doi: <https://doi.org/10.1016/j.jsv.2022.117274>

This is a PDF file of an article that has undergone enhancements after acceptance, such as the addition of a cover page and metadata, and formatting for readability, but it is not yet the definitive version of record. This version will undergo additional copyediting, typesetting and review before it is published in its final form, but we are providing this version to give early visibility of the article. Please note that, during the production process, errors may be discovered which could affect the content, and all legal disclaimers that apply to the journal pertain.

© 2022 Published by Elsevier Ltd.

A Novel General-purpose Three-dimensional Continuously Scanning Laser Doppler Vibrometer System for Full-field Vibration Measurement of a Structure with a Curved Surface

K. Yuan, and W.D. Zhu*

Department of Mechanical Engineering

University of Maryland, Baltimore County

1000 Hilltop Circle

Baltimore, MD 21250

*Corresponding author. Tel: +1 410 455 3394; fax: +1 410 455 1052.

Email addresses: kyuan1@umbc.edu (K. Yuan), wzhu@umbc.edu (W.D. Zhu)

Highlights

- A novel general-purpose 3D CSLDV system to measure 3D vibration is developed.
- 3D full-field ODSs of a turbine blade with a curved surface is measured.
- MAC values between ODSs from 3D CSLDV and 3D SLDV measurements are larger than 95%.
- The 3D CSLDV system can measure 1500 times more points than the 3D SLDV system.
- Test time in 3D CSLDV measurement is less than 1/8 of that in 3D SLDV measurement.

Abstract

Three-dimensional (3D) full-field vibration measurement is significant to structures, especially those with curved surfaces. A triaxial accelerometer and a commercial non-contact 3D scanning laser Doppler vibrometer (SLDV) system are usually used in 3D vibration measurement of a structure. However, the triaxial accelerometer can lead to the mass-loading problem for a light-weight structure, and the 3D SLDV system can take a long time to complete scanning of a structure with a large surface in a step-wise scanning mode. This study proposes a novel general-purpose 3D continuously scanning laser Doppler vibrometer (CSLDV) system to measure 3D full-field vibration of a structure with a curved surface in a non-contact and fast way. The proposed 3D CSLDV system consists of three CSLDVs, a profile scanner, and an external controller, and is experimentally validated by measuring 3D full-field vibration of a turbine blade with a curved surface under sinusoidal excitation and identifying its operating deflection shapes (ODSs). A 3D zig-zag scan path is proposed for scanning the curved surface of the blade based on results from the profile scanner, and scan angles of mirrors in CSLDVs are adjusted based on relations among their laser beams to focus three laser spots at one location, and direct them to continuously and synchronously scan the proposed 3D scan path. A signal processing method that is referred to as the demodulation method is used to identify 3D ODSs of the blade. The first six ODSs from 3D CSLDV measurement have good agreement with those from a commercial 3D SLDV system with modal assurance criterion values larger than 95%. In the experiment, it took the 3D SLDV system about 900 seconds to scan 85 measurement points, and the 3D CSLDV system 115.5 seconds to scan 132,000 points, indicating that the 3D CSLDV system proposed in this study is much more efficient than the 3D SLDV system for measuring 3D full-field vibration of a structure with a curved surface.

Keywords: 3D CSLDV system; turbine blade; curved surface; 3D full-field vibration measurement; ODS

1. Introduction

Three-dimensional (3D) full-field vibration measurement is significant to structures, especially those with curved and complex surfaces such as turbine blades, vehicle bodies, and aircraft wings. Modal tests that obtain vibration components along three axes of a coordinate system can provide more

information and locate defects on more complex structures than those that only obtain single-axis vibration, and can improve the accuracy of their structural health monitoring [1]. 3D full-field vibration can also be used to identify dynamic characteristics of a complex structure and update its finite element (FE) model during structural analysis and product design where vibration must be determined in all its components [2]. A triaxial accelerometer is a common device in a modal test to capture 3D vibration of a structure. However, it has some disadvantages as a contact-type sensor, which include the mass loading effect, the tethering problem, and the sensitivity to electromagnetic interference effect. These effects can be amplified when the test structure has light-weight and multiple triaxial accelerometers are needed [3].

A laser Doppler vibrometer (LDV) was developed to measure vibration of a structure in a non-contact way. A conventional LDV can only capture the velocity response of a fixed point on a structure along a single axis that is parallel to its laser beam. Some investigations focused on extending the conventional LDV to a 3D LDV. Typical ideas include assembling an LDV on an industrial robot arm [4], moving an LDV to three different locations [5], and placing three LDVs at three locations and calibrating angles among their laser beams [6]. By orthogonally mounting two scan mirrors in the conventional LDV, a scanning laser Doppler vibrometer (SLDV) was developed to automate modal tests. O'Malley et al. [7] placed a SLDV on a frame with a multi-axis positioning function to extend it to a 3D SLDV system. Di Maio and Copertaro [8] designed a scanning laser head to extend a single LDV to a six-degree-of-freedom system and experimentally validated it by measuring vibration of a 3D structure and identifying its operational deflection shapes (ODSs). Some investigators developed 3D SLDV systems through moving a single SLDV to three different locations [9, 10]. Commercial 3D SLDV systems, such as Polytec PSV-400 and PSV-500, were developed based on calibration among laser beams from three SLDVs. These 3D SLDV systems have been widely used in engineering, such as 3D vibration measurement of a percussion drill under operating conditions for noise reduction purposes [11], longitudinal vibration measurement of a beam for damage detection [12], FE model validation of a sandwich panel [13] and a wind turbine blade [14], and 3D dynamic strain field measurement of a fan blade [15]. However, it usually takes the 3D SLDV system a long time to obtain high spatial resolution, especially for structures with large surfaces, [1], because laser spots must stay at one measurement point for enough time before they are moved to the next one **to conduct more averages of measurement data when high frequency resolution is needed.**

A continuously scanning laser Doppler vibrometer (CSLDV) was developed by continuously moving the laser spot along a designed scan path on a structure to save test time [16, 17]. The CSLDV can be used to measure transverse vibration of a structure through one-dimensional (1D) or two-dimensional (2D) scan paths [17-19], and dense vibration measured from the CSLDV can be used to detect damage in the structure [20-23]. There is still a scarcity of studies on 3D vibration measurement of a structure using the CSLDV. Weekes and Ewins [24] obtained 3D ODSs of a turbine blade with a curved surface with the CSLDV placed at three different locations. However, it is difficult to ensure that the scan path is the same with the CSLDV placed at the three locations. Also, the 3D vibration measurement system based on the single CSLDV cannot be used to measure transient vibration of a structure and monitor its vibration response in real time. Recently, a novel 3D CSLDV system that consists of three CSLDVs was developed to address the above challenges [25-27]. The system can focus three laser spots at one location through calibration and direct them to continuously and synchronously scan a pre-designed scan path on a structure. The system was experimentally validated by 3D vibration measurements of a beam and a plate, and ODS and mode shape results showed good agreement with those from a commercial 3D SLDV system and FE models. However, the system function was limited to scanning structures with planar surfaces, such as straight beams and flat plates. In the real world, structures can have curved and complex surfaces.

This study aims to propose a novel general-purpose 3D CSLDV system for measuring dense 3D full-field vibration of a structure with a curved surface in a non-contact and fast way. The proposed 3D CSLDV system consists of three CSLDVs, a profile scanner, and an external controller. Calibration among three vibrometer coordinate systems (VCSs) built on the three CSLDVs and a measurement coordinate system (MCS) built on a reference object is conducted to obtain their relations. A 3D scan path can be designed on a curved surface of a structure based on profile scanning, and scan angles of mirrors in CSLDVs can be adjusted based on relations among VCSs and the MCS to focus three laser spots at one location, and direct them to continuously and synchronously scan the proposed 3D scan path. **The laser spot was pre-focused and its size was kept constant during measurement.** A signal processing method for CSLDV measurement that is referred to as the demodulation method [28] is used to identify 3D ODSs of the structure. The system in this study is experimentally validated by measuring 3D vibration components and identifying 3D ODSs of a turbine blade with a curved surface under sinusoidal excitation. Six 3D ODSs of the turbine blade are identified in the experiment.

Comparison between ODSs identified by the proposed 3D CSLDV system and those identified by a commercial 3D SLDV system is made in this study. The minimum modal assurance criterion (MAC) value between them is 95%. The test time in 3D CSLDV measurement is less than 1/8 of that in 3D SLDV measurement, while the number of measurement points in 3D CSLDV measurement is about 1,500 times of that in 3D SLDV measurement.

This work is outlined as follows. The calibration method of the 3D CSLDV system is presented in Sec. 2.1, the 3D scan path design method is presented in Sec. 2.2, and the velocity transformation method is shown in Sec. 2.3. The experimental setup for measuring 3D vibration of a turbine blade with clamped-free boundary conditions is presented in Sec. 3.1, profile scanning and generated mirror signal results are presented in Sec. 3.2, results of velocity transformation are shown in Sec. 3.3, and 3D ODS identification of the turbine blade is presented in Sec 3.4. Conclusions are presented in Sec. 4.

2. 3D CSLDV system for structures with curved surfaces

As shown in Fig. 1, Top, Left, and Right CSLDVs are main devices for capturing vibration in the proposed 3D CSLDV system. Spatial positions of the three CSLDVs with respect to a reference object can be calculated through a calibration process. A 3D scan path on a curved surface of a test structure can be predesigned based on calibration and profile scanning results, and scan angles of mirrors in CSLDVs can be adjusted based on them to focus three laser spots at one location, and direct them to continuously and synchronously scan the proposed 3D scan path. The developed 3D CSLDV system is extended from the commercial Polytec PSV-500-3D system, which can only conduct step-wise scanning, by connecting an external controller to interface connectors in its three laser heads. The Polytec PSV-500-3D system also has an internal profile scanner that can be used to capture 3D coordinates of points on the test structure. The external controller used to design and generate signals for scan mirrors in this study is a dSPACE MicroLabBox. The 3D CSLDV system and Polytec PSV-500-3D system can be easily switched to each other by connecting or disconnecting the MicroLabBox to the systems.

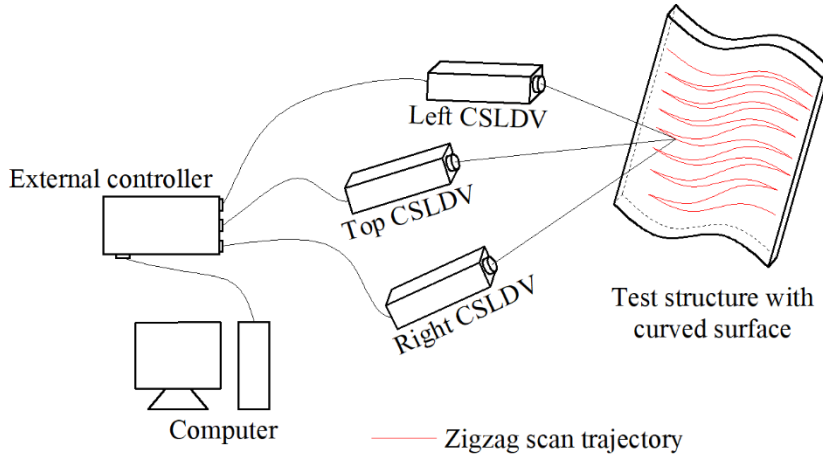


Fig. 1 Schematic of the proposed 3D CSLDV system

2.1 Calibration of the 3D CSLDV system

The 3D CSLDV system can be calibrated by a reference object with known coordinates that is shown in Fig. 2(a). To determine the location of a CSLDV in the system during measurement, a VCS is created based on its two orthogonal scan mirrors (X and Y mirrors). As shown in Fig. 2(b), rotating centers of X and Y mirrors, referred to as o' and o'' , respectively, are located along the same axis $o'z'$ of the VCS $o'-x'y'z'$ with a separation distance d . Rotating axes of the two scan mirrors are $o'x'$ and $o''y''$ axes, respectively, and $o''y''$ and $o'y'$ axes are parallel to each other. Rotating angles of X and Y mirrors, α and β , respectively, can be controlled by the external controller. Note that points M' and o'' on the laser beam path are incident points on X and Y mirrors, respectively. The point o'' is imaged as the point M'' on the plane $y'o'z'$. For a calibrating point M on the reference object, its coordinates in the MCS $\mathbf{M}_{MCS} = [x, y, z]^T$ are known, and its coordinates in the VCS can be determined by

$$\mathbf{M}_{VCS} = [-d \tan(\beta) - s \sin(\beta), -s \cos(\alpha) \cos(\beta), -s \sin(\alpha) \cos(\beta)]^T, \quad (1)$$

where the superscript T represents matrix transpose and s represents the distance between points M and M' . The relation between \mathbf{M}_{MCS} and \mathbf{M}_{VCS} is determined by using a translation vector \mathbf{T} and a direction cosine matrix \mathbf{R} :

$$\mathbf{M}_{MCS} = \mathbf{T} + \mathbf{R} \mathbf{M}_{VCS}, \quad (2)$$

where $\mathbf{T} = [x_{o'}, y_{o'}, z_{o'}]^T$ denotes coordinates of the origin of the VCS o' in the MCS. By solving an optimization problem and an over-determined nonlinear problem [25, 29], \mathbf{T} and \mathbf{R} matrices for all the three CSLDVs can be calculated.

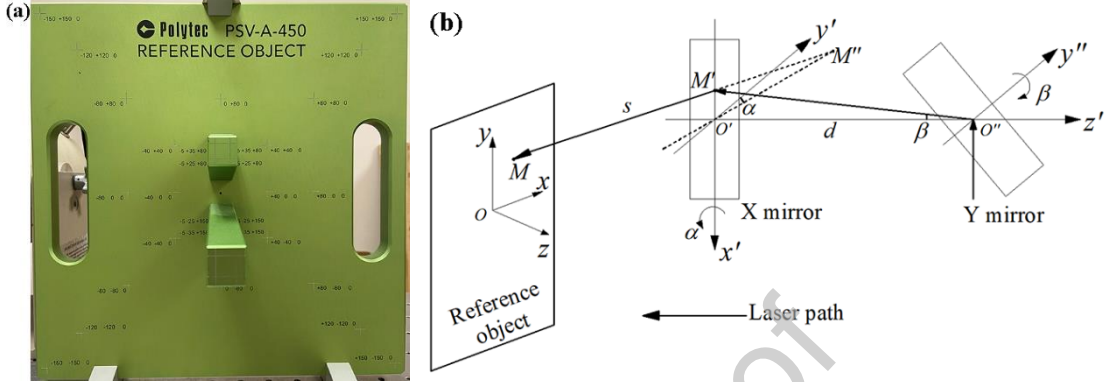


Fig. 2 (a) Reference object used for calibrating the three CSLDVs and (b) the geometric model of the pair of scan mirrors in a CSLDV

2.2 Design of a 3D scan path on a curved surface

An efficient bisection method was developed for designing a straight-line scan path for a beam in Ref. [26], and a 2D zigzag scan path for a flat plate in Ref. [27]. However, the bisection method assumes that all the measurement points are in a plane; so it is not suitable for 3D CSLDV measurement of structures with curved surfaces. In this study, a more general method is developed to address the challenge and design scan paths on both planar and curved surfaces.

As mentioned in Sec. 2.1, the 3D CSLDV system contains three VCSs and one MCS. A measurement point M^k on the surface of a test structure has constant coordinates in the MCS and different coordinates in three VCSs. Therefore, relations among three CSLDVs based on the point is

$$\mathbf{M}_{MCS}^k = \mathbf{T}_1 + \mathbf{R}_1 \mathbf{M}_{VCS_1}^k = \mathbf{T}_2 + \mathbf{R}_2 \mathbf{M}_{VCS_2}^k = \mathbf{T}_3 + \mathbf{R}_3 \mathbf{M}_{VCS_3}^k, \quad (3)$$

where the superscript k is the sequence number of the measurement point along the scan path, and subscripts 1, 2, and 3 denote Top, Left, and Right CSLDVs, respectively. By Eq. (3), one has

$$\mathbf{M}_{VCS_1}^k = \mathbf{R}_1^{-1} (\mathbf{M}_{MCS}^k - \mathbf{T}_1), \quad (4)$$

$$\mathbf{M}_{VCS_2}^k = \mathbf{R}_2^{-1} (\mathbf{M}_{MCS}^k - \mathbf{T}_2), \quad (5)$$

$$\mathbf{M}_{VCS_3}^k = \mathbf{R}_3^{-1} (\mathbf{M}_{MCS}^k - \mathbf{T}_3). \quad (6)$$

Based on calculated coordinates of the point M^k in VCSs, rotating angles of scan mirrors in the three CSLDVs are

$$\begin{aligned}\alpha_1^k &= \arctan\left(z_{VCS_1}^k / y_{VCS_1}^k\right) \\ \beta_1^k &= \arctan\left(x_{VCS_1}^k / \left(y_{VCS_1}^k / \cos(\alpha_1^k) - d\right)\right),\end{aligned}\quad (7)$$

$$\begin{aligned}\alpha_2^k &= \arctan\left(z_{VCS_2}^k / y_{VCS_2}^k\right) \\ \beta_2^k &= \arctan\left(x_{VCS_2}^k / \left(y_{VCS_2}^k / \cos(\alpha_2^k) - d\right)\right),\end{aligned}\quad (8)$$

$$\begin{aligned}\alpha_3^k &= \arctan\left(z_{VCS_3}^k / y_{VCS_3}^k\right) \\ \beta_3^k &= \arctan\left(x_{VCS_3}^k / \left(y_{VCS_3}^k / \cos(\alpha_3^k) - d\right)\right),\end{aligned}\quad (9)$$

respectively.

As discussed above, the key to calculate rotation angles of scan mirrors in the three CSLDVs is to obtain exact coordinates of each measurement point on the scan path in the MCS. Although a device like a 3D scanner can be used to easily obtain the profile of a structure, the Polytec PSV-500-3D system is used in this work to scan the test structure and obtain 3D coordinates of points on its surface, which can reduce possible errors from interaction between the scanner and 3D CSLDV system. Note that a linear interpolation is used to process the obtained surface profile, since the Polytec PSV-500-3D system can only move laser spots in a step-wise mode along a pre-defined grid that is not dense enough to generate signals for CSLDV measurement.

2.3 Velocity transformation from VCSs to the MCS

The relation between velocities of the point M^k that are directly measured by the three CSLDVs and its velocity components in x , y , and z directions of the MCS is

$$\left[V_x^k, V_y^k, V_z^k\right]^T = \left[\left[\mathbf{R}_1 \mathbf{e}_1^k, \mathbf{R}_2 \mathbf{e}_2^k, \mathbf{R}_3 \mathbf{e}_3^k\right]^T\right]^{-1} \left[V_1^k, V_2^k, V_3^k\right]^T, \quad (10)$$

where subscripts x , y , and z denote calculated velocity components in corresponding directions, respectively; subscripts 1, 2, and 3, and the superscript k have the same meanings as those indicated in Sec. 2.2; and the vector $\mathbf{e} = [\sin(\beta), \cos(\alpha)\cos(\beta), \sin(\alpha)\cos(\beta)]^T$ denotes the unit vector of the laser path between points M and M' that is shown in Fig. 2(b). By repeating the above transformation at each point along the designed scan path on the test structure, its 3D full-field vibration can be finally obtained in the MCS. The obtained response can not only be directly used to monitor real-time 3D

vibration of the test structure, but also be processed to identify its 3D ODSs. Steps for measuring 3D full-field vibration of a structure with a curved surface by the 3D CSLDV system described above can be schematized in Fig. 3.

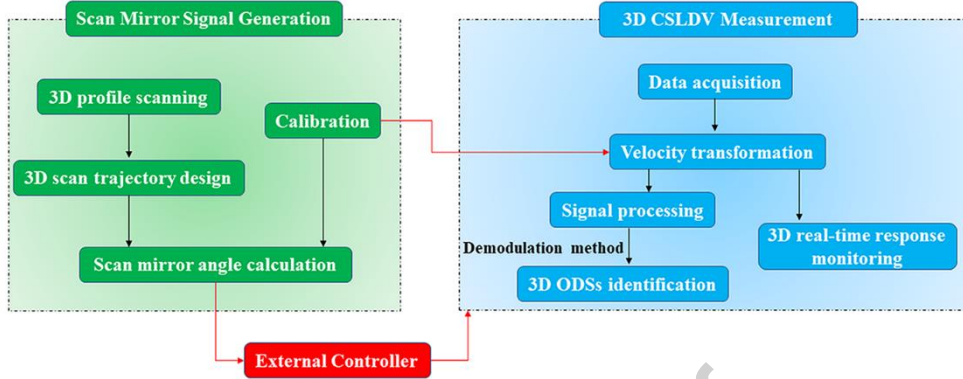


Fig. 3 Schematic of 3D full-field vibration measurement using the proposed 3D CSLDV system

3 Experimental investigation

3.1 Experimental setup

A turbine blade twisted from a trapezoidal plate was used as the test structure in this work. The original trapezoidal plate had two bases of 26 mm and 42 mm, an altitude of 173.9 mm, and a thickness of 3.5 mm. The blade with a curved surface was clamped at its one end by a bench vice to simulate clamped-free boundary conditions, and excited by a MB Dynamics MODAL-50 shaker at its top end through a stinger, as shown in Fig. 4. *While the blade used in this work is relatively flat at the clamped boundary, it is sufficiently curved at its other parts, especially the free boundary, which can be found from Fig. 4.* A grey reflective tape was attached on the surface of the blade to maximize back-scattering of laser light. In the experiment, the MCS was set as parallel to the clamped end of the blade (Fig. 4(b)), so that the z direction represents the out-of-plane component of vibration of the blade, and x and y directions represent its in-plane components. Sinusoidal excitations with different frequencies were used in this study to obtain ODSs of the blade.

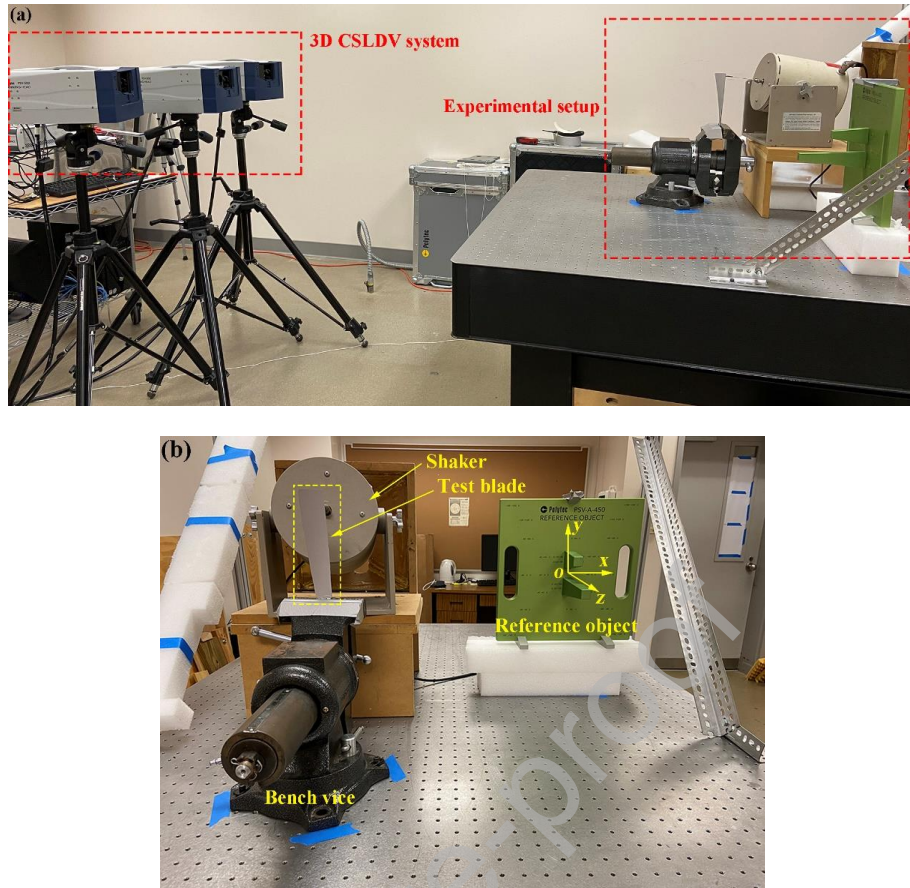


Fig. 4 (a) Arrangement of the 3D CSLDV system and test blade, and (b) the position of the blade in the MCS

3.2 Profile scanning and mirror signal generation

As discussed in Sec. 2, a profile scanning procedure was conducted prior to the scan path design. A total of 85 scanning points were arranged as a 17×5 grid, which were also used as measurement points in 3D SLDV measurement and reference points in comparison with CSLDV measurement results. The 3D view of the blade profile is shown in Fig. 5. The frequency spectrum of the blade obtained from 3D SLDV measurement is shown in Fig. 6 as a black solid line. The first six natural frequencies of the blade, which are 37.5 Hz, 370.5 Hz, 403.3 Hz, 695.1 Hz, 1,870.8 Hz, and 2,226.3 Hz, are identified in the frequency range from 0 to 3,000 Hz and marked by red dashed lines. 3D SLDV and CSLDV measurements of the blade under sinusoidal excitations were conducted in the experiment, where excitation frequencies are close to its first six natural frequencies.

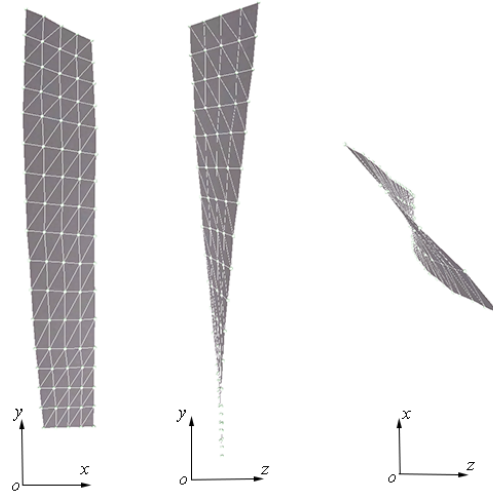


Fig. 5 Profile scanning results of the test blade and its 3D view in the MCS

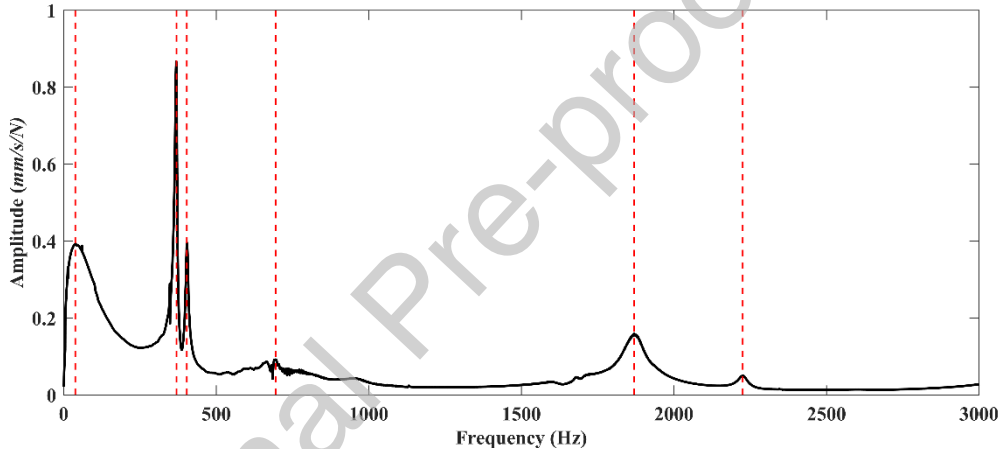


Fig. 6 Frequency spectrum of the test blade shown as a black solid line and its identified natural frequencies shown as red dashed lines by using the 3D SLDV system

Based on profile scanning data and the linear interpolation method, a 3D zig-zag scan path, which includes 33 scan lines, as shown in Fig. 7, was designed for 3D CSLDV measurement of the blade, and coordinates of each point on the scan path were calculated in the MCS. A scanning period T can be defined as a cycle that laser spots move along a scan line from the start point to the end point and move back. The scanning frequency $f_{sca} = 1/T$. In the experiment, $f_{sca} = 1 \text{ Hz}$, and laser spots were designed to move along each scan line with 3.5 periods to ensure continuity of the whole zig-zag scan path and obtain enough response data to conduct a three-time average, **which is the same as that for 3D CSLDV measurement**. Therefore, the total time of scanning the whole blade surface in 3D CSLDV measurement is $t = 33 \times 3.5 \times 1 = 115.5 \text{ s}$. Signals generated for the three CSLDVs are shown in Figs. 8-

10, where two cycles of each signal series are amplified and shown in right subplots. One can see that signals for X mirrors are close to triangular waves, while those for Y mirrors are curved, which are much different from those used for 3D CSLDV measurements of a straight beam [26] and a flat plate [27].

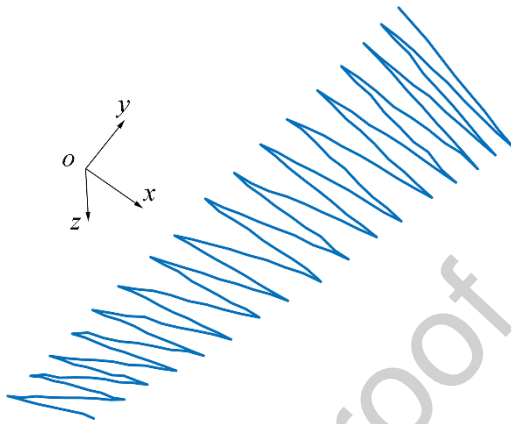


Fig. 7 3D zig-zag scan path designed for 3D CSLDV measurement of the blade

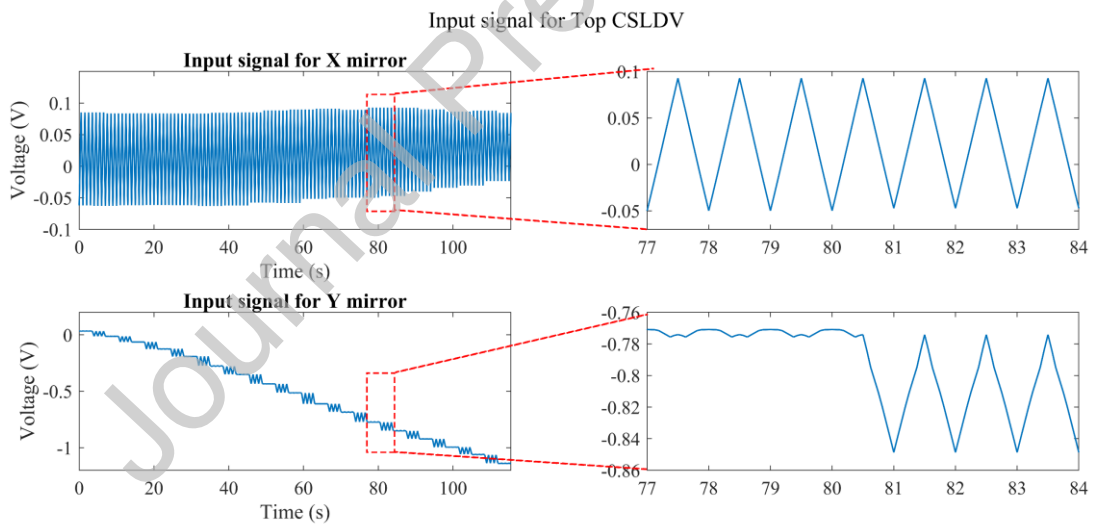


Fig. 8 Input signals for scan mirrors in the Top CSLDV

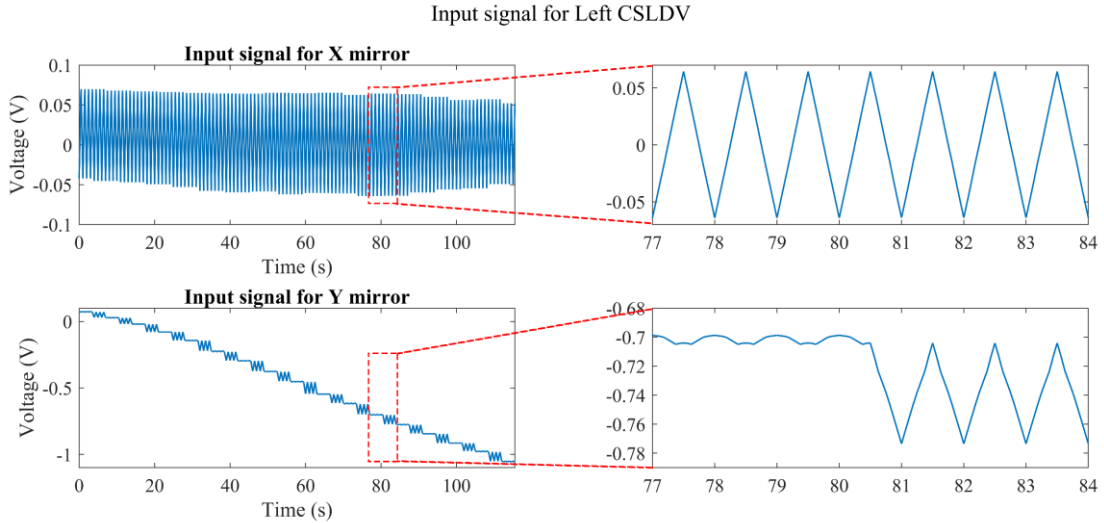


Fig. 9 Input signals for scan mirrors in the Left CSLDV

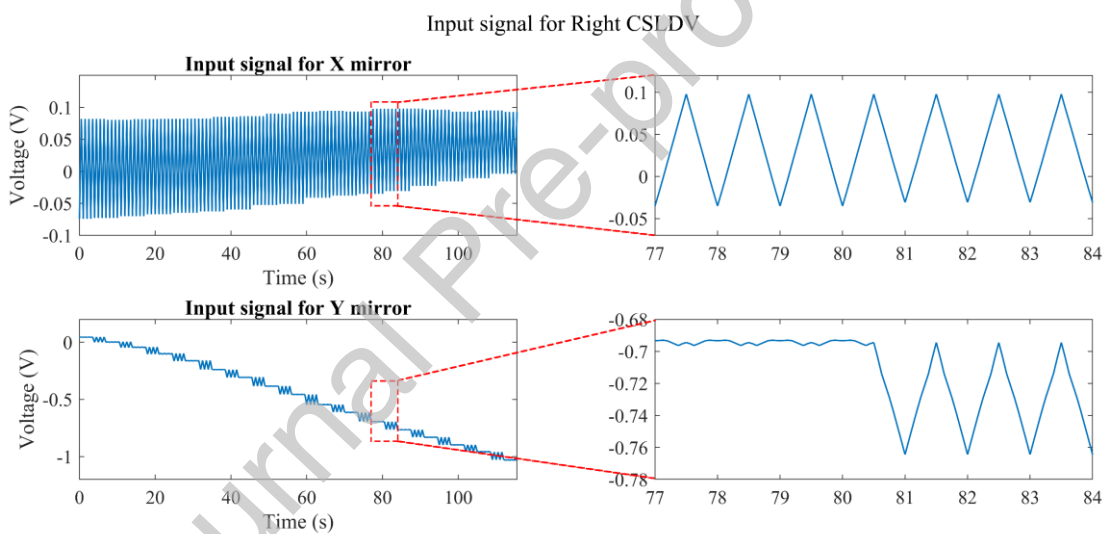


Fig. 10 Input signals for scan mirrors in the Right CSLDV

3.3 Results of velocity transformation

As discussed in Sec. 2.3, vibration of the blade in three VCSs can be directly obtained from 3D CSLDV measurement, while vibration components in the MCS can be obtained through velocity transformation using Eq. (10). In order to indicate the velocity transformation procedure, the original and calculated vibration responses from 3D CSLDV measurements of the blade under sinusoidal excitations with excitation frequencies of 403 Hz and 2,226 Hz are used as two examples, as shown in Figs. 11 and 12, respectively, where horizontal axes represent time and vertical axes represent velocities. In each figure, the three left subplots show original velocities from the three CSLDVs, and

the three right subplots show calculated velocities in three axes of the MCS. In the experiment, laser spots were moved to scan the surface of the blade from its upper end to its lower end; so time-velocity series shown in the two figures represent responses from its free end to its clamped end. One can see that original time-velocity series from the three CSLDV have similar shapes to each other and to calculated velocities in the z direction in the MCS. This is the case because each 1D CSLDV is designed to measure the single-axial velocity along the direction of its laser beam, which is close to the z direction in the experiment. It can also be found that velocities around lower ends of the blade are much smaller than those in other areas, and velocities in the y direction have much smaller amplitudes than those in x and z directions, which are in agreement with theoretically predicted results due to clamped-free boundary conditions of the blade in the experiment.

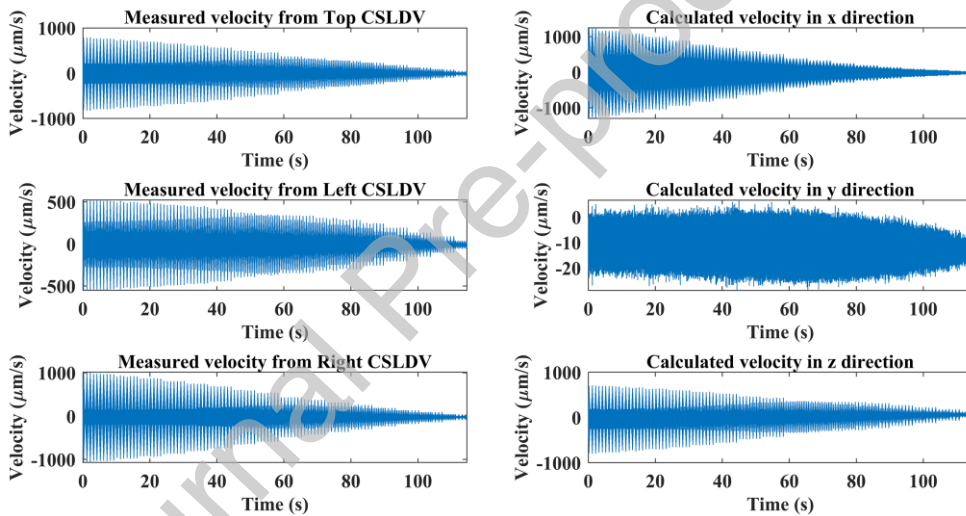


Fig. 11 Transformation from velocities directly obtained by three CSLDV to those in x , y , and z directions in the MCS with the excitation frequency of 403 Hz

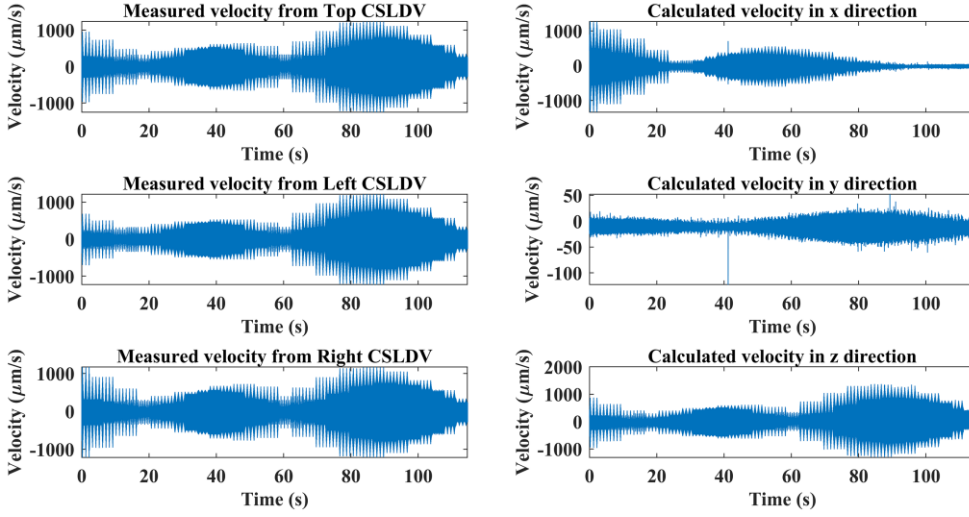


Fig. 12 Transformation from velocities directly obtained by three CSLDV to those in x , y , and z directions in the MCS with the excitation frequency of 2,226 Hz

3.4 Obtaining ODSs using the demodulation method

In this study, the demodulation method [28] was used to process the steady-state response of the blade from 3D CSLDV measurement under sinusoid excitation to obtain its 3D ODSs at various excitation frequencies. The steady-state response u of the blade can be written as

$$u(\mathbf{x}, t) = U(\mathbf{x}) \cos(\omega t - \varphi) = U_I(\mathbf{x}) \cos(\omega t) + U_Q(\mathbf{x}) \sin(\omega t) \quad (11)$$

using the method of separation of variables, where \mathbf{x} and t represent position and time information of measurement points, respectively, φ and ω are the phase and excitation frequency, respectively, and $U(\mathbf{x})$ are responses at measurement points that contain in-phase component $U_I(\mathbf{x})$ and quadrature component $U_Q(\mathbf{x})$. Multiplying $u(\mathbf{x}, t)$ by $\cos(\omega t)$ and $\sin(\omega t)$ yield

$$\begin{aligned} u(\mathbf{x}, t) \cos(\omega t) &= \Phi_I(\mathbf{x}) \cos^2(\omega t) + \Phi_Q(\mathbf{x}) \sin(\omega t) \cos(\omega t) \\ &= \frac{1}{2} \Phi_I(\mathbf{x}) + \frac{1}{2} \Phi_I(\mathbf{x}) \cos(2\omega t) + \frac{1}{2} \Phi_Q(\mathbf{x}) \sin(2\omega t), \end{aligned} \quad (12)$$

$$\begin{aligned} u(\mathbf{x}, t) \sin(\omega t) &= \Phi_I(\mathbf{x}) \sin(\omega t) \cos(\omega t) + \Phi_Q(\mathbf{x}) \sin^2(\omega t) \\ &= \frac{1}{2} \Phi_Q(\mathbf{x}) + \frac{1}{2} \Phi_I(\mathbf{x}) \sin(2\omega t) - \frac{1}{2} \Phi_Q(\mathbf{x}) \cos(2\omega t), \end{aligned} \quad (13)$$

respectively, where $\sin(2\omega t)$ and $\cos(2\omega t)$ terms can be eliminated by a low-pass filter, and $U_I(\mathbf{x})$ and $U_Q(\mathbf{x})$ can be obtained by multiplying filtered responses by a scale factor of two, respectively.

The sampling frequency of 3D CSLDV measurement in the experiment is $f_{sa} = 8,000$ Hz, which is about 3.5 times the sixth natural frequency of the blade shown in Fig. 6 and can cover the frequency range of interest of the blade. The number of sampling points on each scan line of the 3D zig-zag scan path in this study can be obtained using f_{sc} and f_{sa} via

$$k_{each} = 0.5 \times \frac{1}{f_{sc}} \times f_{sa} = 0.5 \times 1 \times 8,000 = 4,000. \quad (14)$$

Therefore, there are a total of 132,000 measurement points on 33 scan lines along the scan path shown in Fig. 7. As shown in Sec. 3.2, the test time of CSLDV measurement is determined by its scanning frequency, number of scanning periods, and density of the scan path. The test time of traditional SLDV measurement is determined by its number of measurement points, frequency resolution, and number of averages. Moreover, it takes some time to move laser spots from one measurement point to the next one. Comparison between the number of measurement points of 3D CSLDV measurement and that of 3D SLDV measurement is shown in the second column in Table 1, and corresponding comparison of the test time is shown in the third column in Table 1. One can see that the number of measurement points in 3D CSLDV measurement is about 1,500 times of that in 3D SLDV measurement, while the test time in 3D CSLDV measurement is less than 1/8 of that in 3D SLDV measurement, meaning that the proposed 3D CSLDV system is much more efficient in 3D full-field vibration measurement than the 3D SLDV system.

Table 1 Comparisons between the number of measurement points and test time of 3D CSLDV measurement and those of 3D SLDV measurement

Measurement system	Number of measurement points	Test time (s)
3D CSLDV system	132,000	115.5
3D SLDV system	85	900

Results of the first six 3D full-field ODSs of the clamped-free blade at six excitation frequencies that are 37 Hz, 370 Hz, 403 Hz, 695 Hz, 1,870 Hz, and 2,226 Hz from 3D SLDV and 3D CSLDV measurements are normalized with unit maximum absolute component values, as shown in Figs. 13-18, where left subplots represent ODSs from SLDV measurement and right subplots represent ODSs from CSLDV measurement. In each subplot, ODSs from x , y , and z directions defined by the MCS are

shown from left to right. One can see that the 1st, 4th, and 6th ODSs from CSLDV measurement are bending modes while the 2nd, 3rd, and 5th ODSs are torsional modes, which have similar patterns to those from corresponding SLDV measurement. It can also be found that ODSs from CSDLV measurement are smoother than those from SLDV measurement, especially for those with higher excitation frequencies, since there are much more measurement points in CSLDV measurement than those in SLDV measurement. Note that ODSs in the *y* direction are less smooth than those in *x* and *z* directions for both SLDV and CSLDV measurements. The possible reason is that longitudinal vibration is harder to be excited than transverse vibration for a cantilever structure, which leads to smaller signal-to-noise ratios (SNRs) in the *y* direction than those in *x* and *z* directions; this can also be validated from 3D real-time responses shown in Figs. 11 and 12.

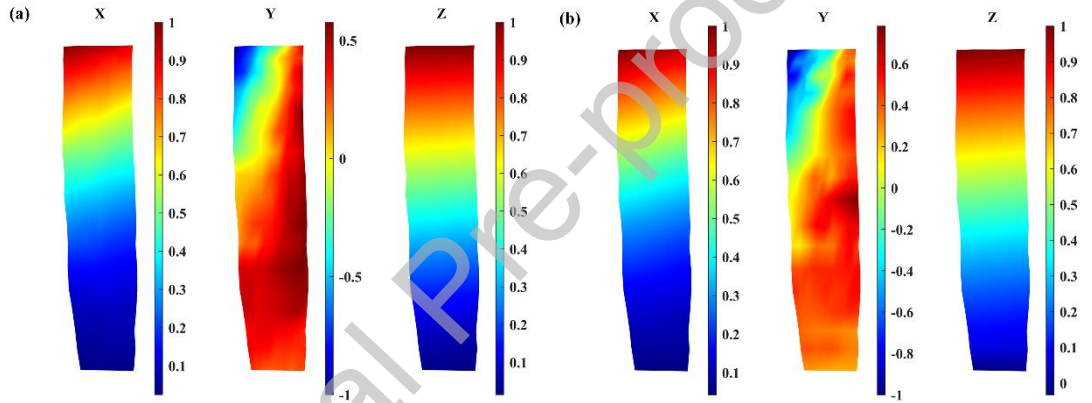


Fig. 13 3D full-field ODSs of the turbine blade from (a) SLDV measurement and (b) CSLDV measurement with the excitation frequency of 37 Hz

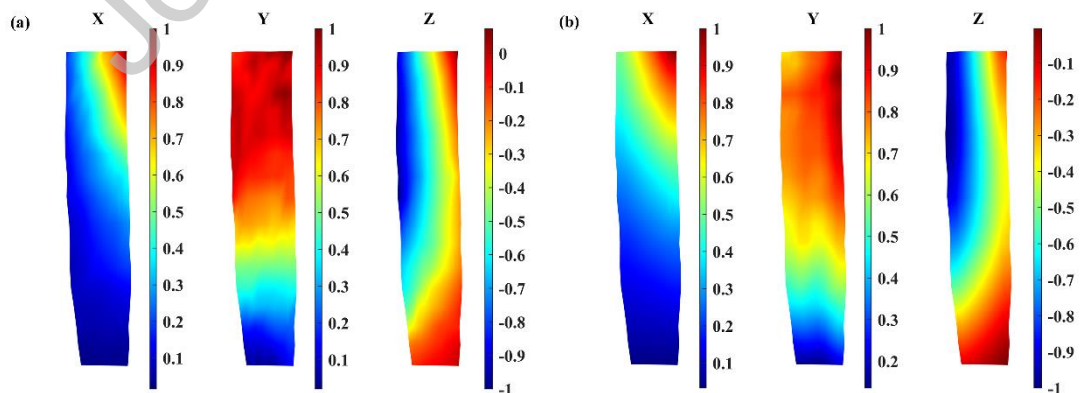


Fig. 14 3D full-field ODSs of the turbine blade from (a) SLDV measurement and (b) CSLDV measurement with the excitation frequency of 370 Hz

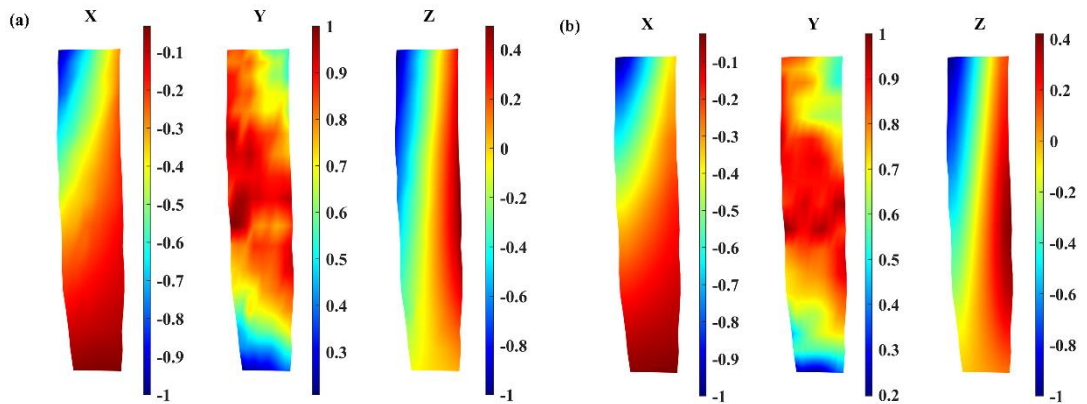


Fig. 15 3D full-field ODSs of the turbine blade from (a) SLDV measurement and (b) CSLDV measurement with the excitation frequency of 403 Hz

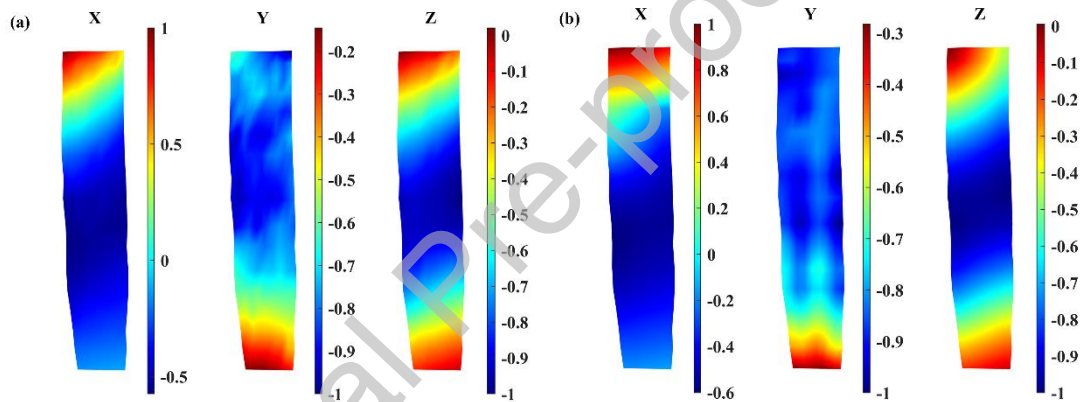


Fig. 16 3D full-field ODSs of the turbine blade from (a) SLDV measurement and (b) CSLDV measurement with the excitation frequency of 695 Hz

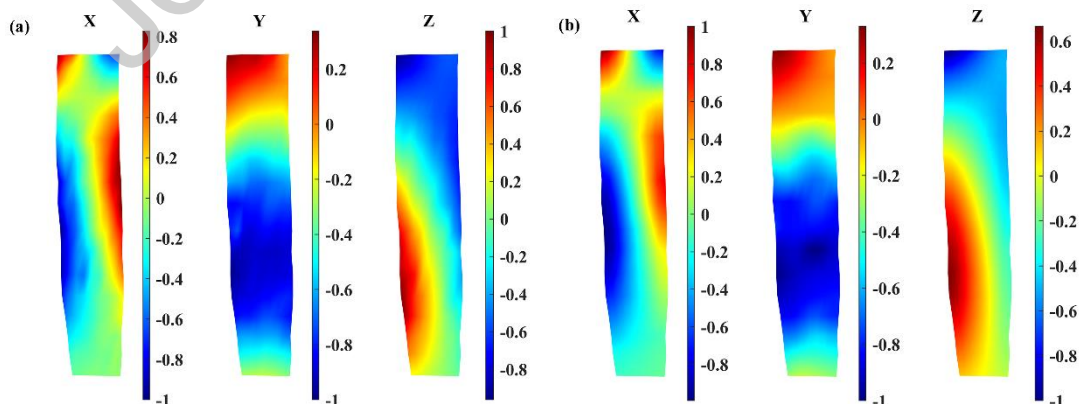


Fig. 17 3D full-field ODSs of the turbine blade from (a) SLDV measurement and (b) CSLDV measurement with the excitation frequency of 1,870 Hz

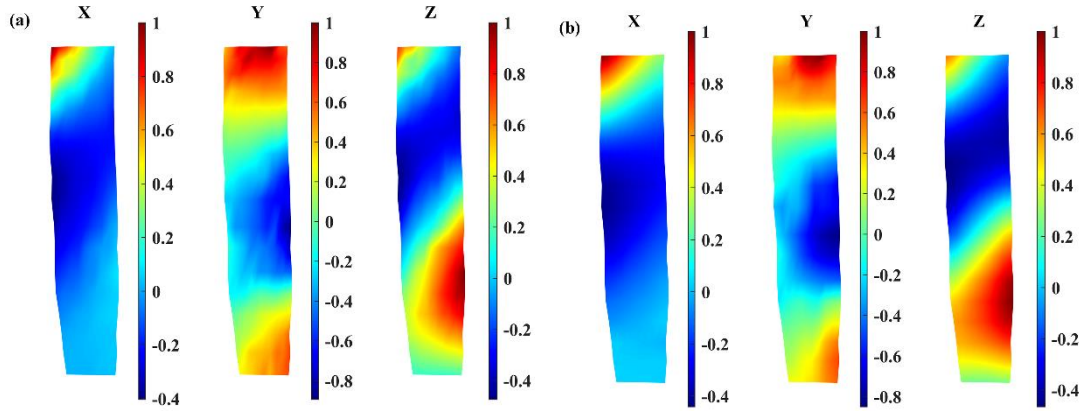


Fig. 18 3D full-field ODSs of the turbine blade from (a) SLDV measurement and (b) CSLDV measurement with the excitation frequency of 2,226 Hz

To further check correlations between 3D full-field ODSs of the turbine blade from 3D SLDV and 3D CSLDV measurements, their MAC values [30] are listed in Table 2. For all the six modes in three directions, one can see that the minimum MAC value is 95%, showing high correlations between results from the commercial 3D SLDV system and proposed 3D CSLDV system. It can be safely concluded that accuracy of the commercial 3D SLDV system and proposed 3D CSLDV system are at the same level.

Table 2 MAC values between 3D full-field ODSs of the turbine blade under sinusoidal excitations from 3D SLDV measurement and those from 3D CSLDV measurement

Mode No.	MAC values		
	<i>x</i>	<i>y</i>	<i>z</i>
1	99.9%	95.2%	99.9%
2	95.6%	97.7%	98.3%
3	99.6%	99.4%	97.3%
4	97.1%	98.0%	99.5%
5	95%	99.4%	96.4%
6	95.4%	96.9%	96.6%

4 Conclusions

A novel general-purpose 3D CSLDV system is developed and experimentally validated through 3D vibration measurement and modal parameter identification of a turbine blade with a curved surface under sinusoidal excitation. Calibration among three VCSs built on the three CSLDVs and a MCS built on a reference object is conducted to obtain their relations. A 3D zig-zag scan path is proposed based on profile scanning, and scan angles of CSLDVs are adjusted based on relations among VCSs and the MCS to focus three laser spots at one location, and direct them to continuously and synchronously scan the proposed 3D scan path. By using sinusoidal excitations with frequencies in the range from 0 to 3,000 Hz to excite the blade, six 3D full-field ODSs of the blade are obtained. Comparison between the first six ODSs from 3D SLDV measurement and those from 3D CSLDV measurement is made in this study. The minimum MAC value between them is 95%, meaning that the proposed 3D CSLDV system has the same accuracy as that of the commercial 3D SLDV system. In the experiment, the number of measurement points in 3D CSLDV measurement is about 1,500 times of that in 3D SLDV measurement, while the test time in 3D CSLDV measurement is less than 1/8 of that in 3D SLDV measurement, meaning that the 3D CSLDV system is much more efficient than the 3D SLDV system for measuring 3D full-field vibration of a structure with a curved surface.

Extending the proposed methodology to estimate 3D mode shapes a structure with a curved surface under random excitation, which is the most practical excitation method, is an important topic for a follow-up study, where development of an extended demodulation method for handling response of a structure under random excitation and enhancement of SNRs of measured response of the structure would be foreseeable challenges. The results will be published in a follow-up work. In addition, the field of view of a structure with a large curvature, such as a cylinder and sphere, can be a common challenge in its vibration measurement using an LDV. The problem can be resolved by using a mirror to extend the field of view so that even vibration of the back side of the structure can be measured without moving the structure or the LDV. The 3D CSLDV system and its calibration and scan path design methods proposed in this study are applicable to vibration measurement of a cylinder and sphere once coordinates of their measurement points are obtained. This would be a case study in some future work.

Credit Author Statement

Ke Yuan: Methodology, Software, Validation, Writing - original draft

Weidong Zhu: Conceptualization, Methodology, Supervision, Funding acquisition, Writing - review & editing

Acknowledgement

This research was supported by the National Science Foundation through Grant No. CMMI-1763024.

References

- [1] S.J. Rothberg, M.S. Allen, P. Castellini, D. Di Maio, J.J.J. Dirckx, D.J. Ewins, B.J. Halkon, P. Muyshondt, N. Paone, T. Ryan, H. Steger, E.P. Tomasini, S. Vanlanduit, J.F. Vignola, An international review of laser Doppler vibrometry: Making light work of vibration measurement, Opt. Lasers Eng., 99 (2017), pp. 11-22. <https://doi.org/10.1016/j.optlaseng.2016.10.023>.
- [2] P. Castellini, M. Martarelli, E.P. Tomasini, Laser Doppler Vibrometry: Development of advanced solutions answering to technology's needs, Mech. Syst. Signal Process., 20 (6) (2006), pp. 1265-1285. <https://doi.org/10.1016/j.ymssp.2005.11.015>.
- [3] J. La, J. Choi, S. Wang, K. Kim, K. Park, Continuous scanning laser Doppler vibrometer for mode shape analysis, Opt. Eng., 42 (3) (2003), pp. 730-737. <https://doi.org/10.1117/1.1533794>.
- [4] P. Margerit, T. Gobin, A. Lebée, J.F. Caron, The robotized laser doppler vibrometer: On the use of an industrial robot arm to perform 3D full-field velocity measurements, Opt. Lasers Eng., 137 (2021), p. 106363. <https://doi.org/10.1016/j.optlaseng.2020.106363>.
- [5] S. Sels, S. Vanlanduit, B. Bogaerts, R. Penne, Three-dimensional full-field vibration measurements using a handheld single-point laser Doppler vibrometer, Mech. Syst. Signal Process., 126 (2019), pp. 427-438. <https://doi.org/10.1016/j.ymssp.2019.02.024>.
- [6] T. Miyashita, Y. Fujino, Development of 3D vibration measurement system using laser doppler vibrometers, in: Health Monitoring and Smart Nondestructive Evaluation of Structural and Biological Systems V, SPIE, 2006, pp. 170-179. <https://doi.org/10.1117/12.662159>.

[7] P. O'Malley, T. Woods, J. Judge, J. Vignola, Five-axis scanning laser vibrometry for three-dimensional measurements of non-planar surfaces. *Meas. Sci. Technol.*, 20 (11) (2009), p. 115901. <http://doi.org/10.1088/0957-0233/20/11/115901>.

[8] D. Di Maio, E. Copertaro, Experimental validation of a newly designed 6 degrees of freedom scanning laser head: application to three-dimensional beam structure, *Rev. Sci. Instrum.*, 84 (12) (2013), p. 121708. <https://doi.org/10.1063/1.4845535>.

[9] D. Kim, H. Song, H. Khalil, J. Lee, S. Wang and K. Park, 3-D vibration measurement using a single laser scanning vibrometer by moving to three different locations, *IEEE Trans. Instrum. Meas.*, 63 (8) (2014), pp. 2028-2033. <https://doi.org/10.1063/1.4845535>.

[10] D.M. Chen, W.D. Zhu, Investigation of three-dimensional vibration measurement by a single scanning laser Doppler vibrometer, *J. Sound Vib.*, 387 (2017), pp. 36-52. <https://doi.org/10.1016/j.jsv.2016.09.026>.

[11] K. Bendel, M. Fischer, M. Schuessler, Vibrational analysis of power tools using a novel three-dimensional scanning vibrometer, in: Sixth International Conference on Vibration Measurements by Laser Techniques: Advances and Applications, SPIE, 2014, pp. 177-184. <https://doi.org/10.1117/12.579525>.

[12] W. Xu, W. D. Zhu, S. A. Smith, M. S. Cao, Structural damage detection using slopes of longitudinal vibration shapes, *J. Vib. Acoust.*, 138 (3) (2016), p. 034501. <https://doi.org/10.1115/1.4031996>.

[13] K. Yuan, W. Zhu, Modeling of welded joints in a pyramidal truss sandwich panel using beam and shell finite elements, *J. Vib. Acoust.*, 143 (4) (2021), p. 041002. <https://doi.org/10.1115/1.4048792>.

[14] Y. Chen, A.S. Mendoza, D.T. Griffith, Experimental and numerical study of high-order complex curvature mode shape and mode coupling on a three-bladed wind turbine assembly, *Mech. Syst. Signal Process.*, 160 (2021), p. 107873. <https://doi.org/10.1016/j.ymssp.2021.107873>.

[15] C. Vuye, S. Vanlanduit, F. Presezniak, G. Steenackers, P. Guillaume, Optical measurement of the dynamic strain field of a fan blade using a 3D scanning vibrometer, *Opt. Lasers Eng.*, 49 (7) (2011), pp. 988-997. <https://doi.org/10.1016/j.optlaseng.2011.01.021>.

[16] B.J. Halkon, S.R. Frizzel, S.J. Rothberg, Vibration measurements using continuous scanning laser vibrometry: velocity sensitivity model experimental validation, *Meas. Sci. Technol.*, 14 (6)

(2003), pp. 773-783. <https://doi.org/10.1088/0957-0233/14/6/310>.

[17] D. Di Maio, P. Castellini, M. Martarelli, S. Rothberg, M.S. Allen, W.D. Zhu, D.J. Ewins, Continuous Scanning Laser Vibrometry: A raison d'être and applications to vibration measurements. *Mech. Syst. Signal Process.*, 156 (2021), p. 107573. <https://doi.org/10.1016/j.ymssp.2020.107573>.

[18] L.F. Lyu, W.D. Zhu, Operational modal analysis of a rotating structure under ambient excitation using a tracking continuously scanning laser Doppler vibrometer system, *Mech. Syst. Signal Process.*, 152 (2021), p. 107367. <https://doi.org/10.1016/j.ymssp.2020.107367>.

[19] L.F. Lyu, W.D. Zhu, Full-field mode shape estimation of a rotating structure subject to random excitation using a tracking continuously scanning laser Doppler vibrometer via a two-dimensional scan scheme, *Mech. Syst. Signal Process.*, 169 (2022), p. 108532. <https://doi.org/10.1016/j.ymssp.2021.108532>.

[20] D.M. Chen, Y.F. Xu, W.D. Zhu, Damage identification of beams using a continuously scanning laser doppler vibrometer system, *J. Vib. Acoust.*, 138 (5) (2016), p. 051011. <https://doi.org/10.1115/1.4033639>.

[21] D.M. Chen, Y.F. Xu, W.D. Zhu, Experimental investigation of notch-type damage identification with a curvature-based method by using a continuously scanning laser doppler vibrometer system, *J. Nondestruct. Eval.*, 36 (2017), p. 38. <https://doi.org/10.1007/s10921-017-0418-4>.

[22] D.M. Chen, Y.F. Xu, W.D. Zhu, Identification of damage in plates using full-field measurement with a continuously scanning laser Doppler vibrometer system, *J. Sound Vib.*, 422 (2018), pp. 542-567. <https://doi.org/10.1016/j.jsv.2018.01.005>.

[23] Y.F. Xu, D.M. Chen, W.D. Zhu, Operational modal analysis using lifted continuously scanning laser Doppler vibrometer measurements and its application to baseline-free structural damage identification, *J. Vib. Control*, 25 (7) (2019), pp. 1341-1364. <https://doi.org/10.1177/1077546318821154>.

[24] B. Weekes, D. Ewins, Multi-frequency, 3D ODS measurement by continuous scan laser Doppler vibrometry, *Mech. Syst. Signal Process.*, 58-59 (2015), pp. 325-339. <https://doi.org/10.1016/j.ymssp.2014.12.022>.

[25] D.M. Chen, W.D. Zhu, Investigation of three-dimensional vibration measurement by three scanning laser Doppler vibrometers in a continuously and synchronously scanning mode, *J. Sound*

Vib., 498 (2021) p. 115950. <https://doi.org/10.1016/j.jsv.2021.115950>.

[26] K. Yuan, W.D. Zhu, Estimation of modal parameters of a beam under random excitation using a novel 3D continuously scanning laser Doppler vibrometer system and an extended demodulation method, *Mech. Syst. Signal Process.*, 155 (2021), p. 107606. <https://doi.org/10.1016/j.ymssp.2021.107606>.

[27] K. Yuan, W.D. Zhu, In-plane operating deflection shape measurement of an aluminum plate using a three-dimensional continuously scanning laser Doppler vibrometer system, *Exp. Mech.*, 62 (2022), p. 667-676. <https://doi.org/10.1007/s11340-021-00801-x>.

[28] A.B. Stanbridge, D.J. Ewins, Modal testing using a scanning laser Doppler vibrometer, *Mech. Syst. Signal Process.*, 13 (2) (1999), pp. 255-270. <https://doi.org/10.1006/mssp.1998.1209>.

[29] K.S. Arun, T.S. Huang, S.D. Blostein, Least-squares fitting of two 3-D point sets, *IEEE Trans. Pattern Anal. Mach. Intell.*, 9(5) (1985), pp. 698-700. 10.1109/TPAMI.1987.4767965.

[30] D.J. Ewins, *Modal Testing: Theory, Practice and Application*, second ed., Research Studies Press LTD, Hertfordshire, 2000.